Design of brushless DC position servo systems using integral variable structure approach

T.-L. Chern
Y.-C. Wu

Indexing terms: Brushless DC servo motor, Integral-compensated variable structure control, Plant parameter variations

Abstract: This paper considers brushless DC position control systems with unknown external load disturbance and plant parameter variations. Since the dynamic characteristics of such systems are very complex and highly nonlinear, a conventional linear controller design may not assure satisfactory requirements. To improve the dynamic response of such systems, an integral-compensated variable structure control (IVSC) has been proposed. The approach comprises an integral controller for achieving a zero steady-state error response under step input, and a variable structure controller for enhancing the robustness. Simulation results show that the proposed approach gives a rather accurate servo-tracking result and is fairly robust to plant parameter variations and external load disturbance.

1 Introduction

The advantages of brushless DC motors include higher torque/weight ratio, lower rotor moment of inertia, better heat dissipation, smaller size and lower weight as compared to permanent magnet stator DC commutator motors having same output capacity. Thus the brushless DC servo motor is preferable for certain high performance applications such as machine tools, industrial robots and aerospace actuators. The proposed scheme for a brushless DC position servo control system, as shown in Fig. 1, consists of an inner loop for inverter switching and an outer loop for generating the command for the inner loop [1]. The inner loop is a sinusoidal current-controlled pulse width modulated (PWM) voltage-source inverter (VSI) which is, as shown in Fig. 2, widely applied in high performance AC drives. The outer loop is designed to achieve a fast and accurate servo-tracking response under load disturbance and plant parameter variations. However, such requirements are usually difficult to achieve by using a simple linear controller. In certain cases, the variable structure control (VSC) is applied but it may result in a steady-state error when there is load disturbance [4]. This motivates the use of an additional integral action to the conventional VSC design, as has been proposed previously in [5, 6] where successful applications to electrohydraulic servo control systems and robots were achieved. Performance comparison of the proposed approach with the conventional VSC and the linear approaches has been given for an illustration.

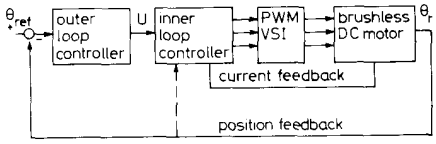

Fig. 1 *Brushless DC servo control structure*

2 Modelling of brushless DC servo motor

The brushless DC servo motor considered in the paper is a three-phase permanent-magnet synchronous motor with sinusoidal back EMF. The stator windings are identical, displaced by 120° and sinusoidally distributed. The voltage equations for the stator windings can be expressed as

$$\begin{bmatrix} v_{as} \\ v_{bs} \\ v_{cs} \end{bmatrix} = \begin{bmatrix} R & 0 & 0 \\ 0 & R & 0 \\ 0 & 0 & R \end{bmatrix} \begin{bmatrix} i_{as} \\ i_{bs} \\ i_{cs} \end{bmatrix} + \frac{d}{dt} \begin{bmatrix} L_a & L_{ba} & L_{ca} \\ L_{ba} & L_b & L_{cb} \\ L_{ca} & L_{cb} & L_c \end{bmatrix} \begin{bmatrix} i_{as} \\ i_{bs} \\ i_{cs} \end{bmatrix} + \omega_r \lambda_m \begin{bmatrix} \sin(\theta_r) \\ \sin(\theta_r - 2\pi/3) \\ \sin(\theta_r + 2\pi/3) \end{bmatrix} \quad (1a)$$

where

v_{as}, v_{bs}, v_{cs} = the applied stator voltages
i_{as}, i_{bs}, i_{cs} = the applied stator currents
R = the resistance of each stator winding
L_a, L_b, L_c = the self inductances of the stator windings
L_{ba}, L_{ca}, L_{cb} = the mutual inductances of the stator windings
ω_r = the electrical rotor angular velocity
θ_r = the electrical rotor angular displacement, which is defined as the angle between the d-axis (fixed at the center of the north pole of the permanent magnet rotor) and the phase a axis of the stator
λ_m = the amplitude of the flux linkage established by the permanent magnet as viewed from the stator windings

Paper 9052B (P1), first received 9th October 1991 and in revised form 23rd June 1992

T.-L. Chen is with the Department of Electrical Engineering, National Sun Yat-Sen University, Kaohsiung, Taiwan 80424, Republic of China

Y.-C. Wu is with the Institute of Control Engineering, National Chiao Tung University, Hsinchu, Taiwan, Republic of China

Assume that the airgap and the rotor construction of the permanent synchronous machine are uniform, then

$$L_a = L_b = L_c = L$$

$$L_{ba} = L_{ca} = L_{cb} = M$$

Thus, eqn. 1*a* can be rewritten as follows:

$$\begin{bmatrix} v_{as} \\ v_{bs} \\ v_{cs} \end{bmatrix} = \begin{bmatrix} R & 0 & 0 \\ 0 & R & 0 \\ 0 & 0 & R \end{bmatrix} \begin{bmatrix} i_{as} \\ i_{bs} \\ i_{cs} \end{bmatrix} + \frac{d}{dt} \begin{bmatrix} L & M & M \\ M & L & M \\ M & M & L \end{bmatrix} \begin{bmatrix} i_{as} \\ i_{bs} \\ i_{cs} \end{bmatrix} + \omega_r \lambda_m \begin{bmatrix} \sin(\theta_r) \\ \sin(\theta_r - 2\pi/3) \\ \sin(\theta_r + 2\pi/3) \end{bmatrix} \quad (1b)$$

Substitution of $i_{as} + i_{bs} + i_{cs} = 0$ into eqn. 1*b* yields

$$\begin{bmatrix} v_{as} \\ v_{bs} \\ v_{cs} \end{bmatrix} = \begin{bmatrix} R & 0 & 0 \\ 0 & R & 0 \\ 0 & 0 & R \end{bmatrix} \begin{bmatrix} i_{as} \\ i_{bs} \\ i_{cs} \end{bmatrix} + \frac{d}{dt} \begin{bmatrix} L-M & 0 & 0 \\ 0 & L-M & 0 \\ 0 & 0 & L-M \end{bmatrix} \begin{bmatrix} i_{as} \\ i_{bs} \\ i_{cs} \end{bmatrix} + \omega_r \lambda_m \begin{bmatrix} \sin(\theta_r) \\ \sin(\theta_r - 2\pi/3) \\ \sin(\theta_r + 2\pi/3) \end{bmatrix} \quad (1c)$$

The electromagnetic torque can be expressed as [7]

$$T_e = \frac{P}{2} \lambda_m \left[i_{as} \sin(\theta_r) + i_{bs} \sin\left(\theta_r - \frac{2\pi}{3}\right) + i_{cs} \sin\left(\theta_r + \frac{2\pi}{3}\right) \right] \quad (2a)$$

where P is the number of poles.

The torque, velocity and position may be related by:

$$T_e = J\left(\frac{2}{P}\right) \frac{d\omega_r}{dt} + B_m\left(\frac{2}{P}\right)\omega_r + T_L \quad (2b)$$

$$\theta_r = \int \omega_r \, dt \quad (2c)$$

$$\theta_m = \theta_r\left(\frac{2}{P}\right) \quad (2d)$$

where J is the inertia of the rotor, B_m is a damping coefficient, T_L is the load torque, and θ_m is the mechanical angular position of rotor.

The block diagram of a brushless DC machine, portraying eqns. 1*c* and 2, is shown in Fig. 3.

3 The integral variable structure system (IVSS)

A single input IVSS for tracking an input command r with the presence of external disturbance is considered in this paper. The proposed IVSC configuration comprises

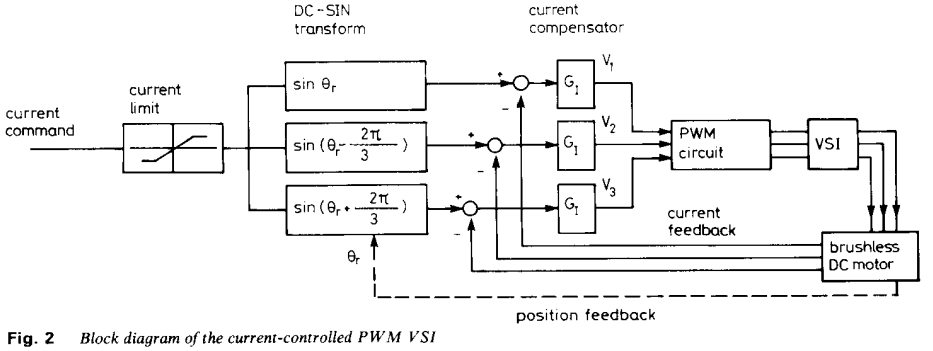

Fig. 2 *Block diagram of the current-controlled PWM VSI*

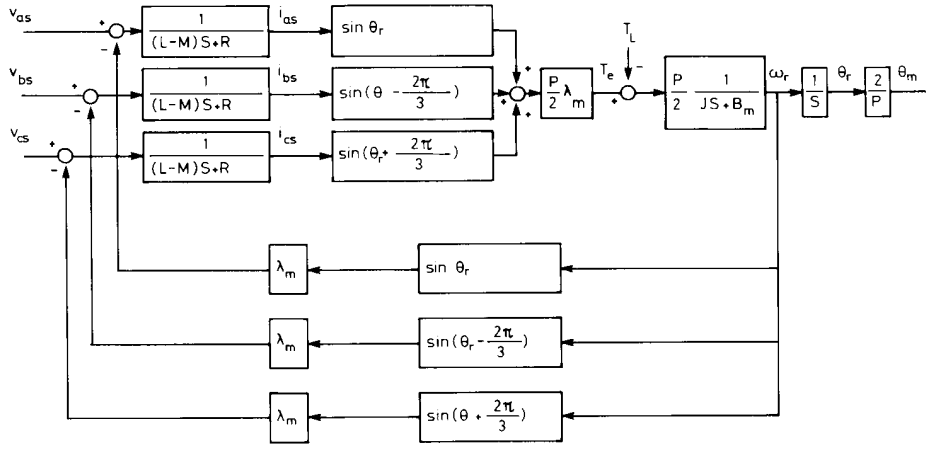

Fig. 3 *Block diagram of the brushless DC motor*

an integral controller and a variable structure controller as shown in Fig. 4 and is described as [5]:

$$\dot{X}_i = X_{i+1} \quad i = 1, \ldots, n-1 \tag{3a}$$

$$\dot{X}_n = -\sum_{i=1}^{n} a_i X_i + bU - f(t) \tag{3b}$$

$$\dot{Z} = r - X_1 \tag{3c}$$

where X_1 is the output signal, r is the input command, K_I is the gain of the integral controller, a_i and b are the

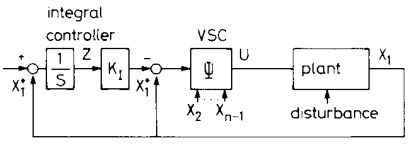

Fig. 4 *Block diagram of an integral variable structure control system*

plant parameters, and $f(t)$ is the disturbance. The control function, U, is a piecewise linear function of the form

$$U = \begin{cases} U^+(x, t) & \text{if } \sigma > 0 \\ U^-(x, t) & \text{if } \sigma < 0 \end{cases} \tag{4}$$

where σ is the switching function, given by

$$\sigma = c_1(X_1 - K_I Z) + \sum_{i=2}^{n} c_i X_i \quad c_i = \text{constant } c_n = 1 \tag{5}$$

The design of such a system involves

(i) the choice of the control function U to guarantee the existence of a sliding mode

(ii) the determination of the switching function σ and the integral control gain K_I such that the system has the desired eigenvalues

(iii) the elimination of chattering of the control signal.

3.1 Choice of the control function

From eqns. 3 and 5, one has

$$\dot{\sigma} = -c_1 K_I(r - X_1) + \sum_{i=2}^{n} c_{i-1} X_i - \sum_{i=1}^{n} a_i X_i + bU - f(t) \tag{6}$$

Let

$$a_i = a_i^0 + \Delta a_i \quad i = 1, \ldots, n$$

$$b = b^0 + \Delta b$$

where a_i^0 and b^0 are the nominal values, and Δa_i and Δb are the associated variations.

Let the control function U be decomposed into

$$U = U_{eq} + \Delta U \tag{7a}$$

here U_{eq}, called the equivalent control, is defined as the solution of the problem $\dot{\sigma} = 0$ under $f(t) = 0$, $a_i = a_i^0$, $b = b^0$. That is

$$U_{eq} = \left[c_1 K_I(r - X_1) - \sum_{i=2}^{n} c_{i-1} X_i + \sum_{i=1}^{n} a_i^0 X_i \right] \Big/ b^0 \tag{7b}$$

In the sliding motion, $\sigma = 0$, one can obtain

$$X_n = \left[-c_1(X_1 - K_I Z) - \sum_{i=2}^{n-1} c_i X_i \right] \tag{7c}$$

Substitution of eqn. 7c into eqn. 7b yields

$$U_{eq} = \left\{ c_1 K_I(r - X_1) - \sum_{i=2}^{n-1} c_{i-1} X_i + \sum_{i=1}^{n-1} a_i^0 X_i + (c_{n-1} - a_n^0) \times \left[c_1(X_1 - K_I Z) + \sum_{i=2}^{n-1} c_i X_i \right] \right\} \Big/ b^0 \tag{7d}$$

The function ΔU, employed to eliminate the influence due to Δa_i, Δb and $f(t)$ so as to guarantee the existence of a sliding mode, is constructed as

$$\Delta U = \Psi_1(X_1 - K_I Z) + \sum_{i=2}^{n} \Psi_i X_i \tag{7e}$$

where

$$\Psi_1 = \begin{cases} \alpha_1 & \text{if } (X_1 - K_I Z)\sigma > 0 \\ \beta_1 & \text{if } (X_1 - K_I Z)\sigma < 0 \end{cases}$$

and

$$\Psi_i = \begin{cases} \alpha_i & \text{if } X_i \sigma > 0 \\ \beta_i & \text{if } X_i \sigma < 0 \end{cases} \quad i = 1, \ldots, n$$

It is known that the condition for the existence and reachability of a sliding motion is [2–4]

$$\sigma\dot{\sigma} < 0 \tag{8}$$

Substitution of eqn. 7 into eqn. 6 yields

$$\begin{aligned} \dot{\sigma} &= -\sum_{i=1}^{n} \Delta a_i X_i - f(t) + (c_{n-1} - a_n) X_n + (c_{n-1} - a_n^0) \\ &\quad \times \left[c_1(X_1 - K_I Z) + \sum_{i=2}^{n-1} c_i X_i \right] + \Delta b U_{eq} + b\,\Delta U \\ &= -\sum_{i=1}^{n} \Delta a_i X_i - f(t) + (c_{n-1} - a_n) X_n + (c_{n-1} - a_n^0) \\ &\quad \times \left[c_1(X_1 - K_I Z) + \sum_{i=2}^{n-1} c_i X_i \right] + \frac{\Delta b}{b^0} \\ &\quad \times \left\{ c_1 K_I(r - X_1) - \sum_{i=2}^{n-1} c_{i-1} X_i + \sum_{i=1}^{n-1} a_i^0 X_i \right. \\ &\quad \left. + (c_{n-1} - a_n^0) \left[c_1(X_1 - K_I Z) + \sum_{i=2}^{n-1} c_i X_i \right] \right\} \\ &\quad + b \left[\Psi_1(X_1 - K_I Z) + \sum_{i=2}^{n} \Psi_i X_i \right] \end{aligned} \tag{9}$$

Then

$$\begin{aligned} \dot{\sigma}\sigma &= [-\Delta a_1 + a_1^0\,\Delta b/b^0 + c_1(c_{n-1} - a_n^0)(1 + \Delta b/b^0) \\ &\quad + b\Psi_1](X_1 - K_I Z)\sigma \\ &\quad + \sum_{i=2}^{n} \{[-\Delta a_i + a_i^0\,\Delta b/b^0 - c_{i-1}\,\Delta b/b^0 \\ &\quad + c_i(c_{n-1} - a_n^0)(1 + \Delta b/b^0) + b\Psi_i] X_i \sigma\} \\ &\quad + N(t) \end{aligned} \tag{10}$$

where

$$\begin{aligned} N(t) = \{ &-K_I Z(\Delta a_1 - a_1^0\,\Delta b/b^0) \\ &+ \Delta b/b^0[c_1 K_I(r - X_1)] - f(t)\}\sigma \end{aligned}$$

If the term $N(t)$ in eqn. 10 is neglected, then the conditions for satisfying inequality 8 are

$$\Psi_i = \begin{cases} \alpha_i < [\Delta a_i - a_i^0\,\Delta b/b^0 + c_{i-1}\,\Delta b/b^0 \\ \qquad - c_i(c_{n-1} - a_n^0)(1 + \Delta b/b^0)]/b \\ \beta_i > [\Delta a_i - a_i^0\,\Delta b/b^0 + c_{i-1}\,\Delta b/b^0 \\ \qquad - c_i(c_{n-1} - a_n^0)(1 + \Delta b/b^0)]/b \end{cases} \quad (11a)$$

for $i = 1, \ldots, n-1$ and $c_0 = 0$, and

$$\Psi_n = \begin{cases} \alpha_n < (\Delta a_n + a_n - c_{n-1})/b \\ \beta_n > (\Delta a_n + a_n - c_{n-1})/b \end{cases} \quad (11b)$$

for $c_0 = 0$.

However, the term $N(t)$ may not be neglected in the presence of input commands, plant parameter variations and/or external disturbance. Hence once the effect of the term $N(t)$ exceeds the sum of other terms in eqn. 10 such that inequality 8 is violated, then the sliding mode breaks down and the system gives rise to a limit cycle. Fortunately, by increasing the control gain Ψ_i, the effect due to the term $N(t)$ can be arbitrarily suppressed so that the magnitude of the limit cycle can be reduced to within a tolerable range, the validity of the assumption can be shown by the simulation, and a quasi-ideal sliding motion can be obtained.

3.2 Determination of the switching plane and integral control gain

When in sliding motion, the system described by eqn. 3 can be reduced to the following linear equations:

$$\dot{X}_i = X_{i+1} \quad i = 1, \ldots, n-2 \quad (12a)$$

$$\dot{X}_{n-1} = -\sum_{i=1}^{n-1} c_i X_i + c_1 K_I Z \quad (12b)$$

$$\dot{Z} = r - X_1 \quad (12c)$$

The closed-loop system (eqns. 12) has a transfer function

$$H(S) = \frac{X_1(S)}{R(S)} = \frac{c_1 K_I}{S^n + c_{n-1}S^{n-1} + \cdots + c_1 S + c_1 K_I} \quad (13)$$

where $R(S)$ and $X_1(S)$ are the Laplace transforms of r and X_1, respectively. Thus, it is obvious that the system shall give a zero steady-state error (with step input) and, because the characteristic equation

$$S^n + c_{n-1}S^{n-1} + \cdots + c_2 S^2 + c_1 S + c_1 K_I = 0 \quad (14)$$

is independent of the plant parameters, it is robust to the plant parameter variations. It is also clear that the eigenvalues can be set arbitrarily by choosing the values of c_1, $\ldots$, c_{n-1} and K_I. Let the desired characteristic equation be

$$S^n + \alpha_1 S^{n-1} + \cdots + \alpha_n = 0 \quad (15)$$

Then c_i and K_I can be chosen as

$$c_{n-1} = \alpha_1$$
$$\vdots$$
$$c_1 = \alpha_{n-1}$$

and

$$K_I = \alpha_n/\alpha_{n-1}$$

3.3 Chattering considerations

For the control law as given by eqn. 7, if Ψ_i, $i = 1, \ldots, n$, are chosen as

$$\Psi_i = \alpha_i = -\beta_i$$

then the control function U can be represented as

$$U = \left\{ c_1 K_I(r - X_1) - \sum_{i=2}^{n-1} c_{i-1} X_i + \sum_{i=1}^{n-1} a_i^0 X_i + (c_{n-1} - a_n^0)\left[c_1(X_1 - K_I Z) + \sum_{i=2}^{n-1} c_i X_i \right] \right\} \Big/ b^0 + \left(\Psi_1 |X_1 - K_I Z| + \sum_{i=2}^{n} \Psi_i |X_i| \right) \text{sign}(\sigma) \quad (16)$$

Since the control U contains the sign function sign (σ), direct application of such a control signal to the plant may give rise to chatterings. To reduce the chatterings, the sign function sign (σ) in eqn. 16 can be replaced by a modified proper continuous function [5] as

$$M_\delta(\sigma) = \frac{\delta}{|\sigma| + \delta} \quad (17)$$

where δ is chosen as a function of $|X_1 - r|$ as

$$\delta = \delta_0 + \delta_1 |X_1 - r|$$

and the value of δ_0 and δ_1 are positive constants.

4 The brushless DC servo position control problem

The objective of the control is to keep the mechanical angular position, θ_m, of the rotor to follow the desired trajectory, θ_c, as closely as possible, regardless of the operating points. The block diagram of the brushless DC position servo control system is shown in Fig. 5. This scheme contains a brushless DC motor, a power driver and the IVSC. In the following, the motor driver and the design of IVSC will be described.

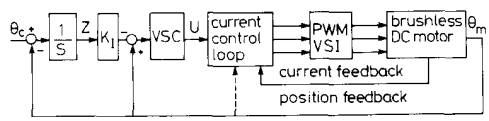

Fig. 5 *Block diagram of an integral variable structure brushless DC servo position control system*

4.1 The motor driver

In this paper, the motor driver is a sinusoidal current controlled PWM voltage source inverter (VSI), as shown in Fig. 2, consisting of the DC–SIN transform, current compensator, and PWM and VSI circuits. The DC–SIN transform circuit is employed to transform the reference current command into the three phase sinusoidal current commands and the current compensator G_I is designed to achieve fast accurate current tracking. The function of the PWM circuit is shown in Fig. 6, where $V_i (i = 1, 2, 3)$ is the phase driver signal (which also appears in Fig. 2)

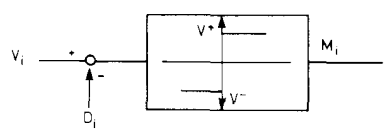

Fig. 6 *The function block of the PWM circuit*

and D_i ($i = 1, 2, 3$) is the high frequency triangular signal (in the range from 1 to 50 kHz). The compared result between the V_i and D_i is used to control the switching signal $M_i(i = 1, 2, 3)$ which, in turn, determines the ON/OFF state of the power transistors ($T_1 \sim T_6$) in the VSI as shown in Fig. 7.

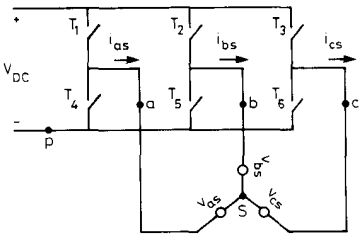

Fig. 7 *The power circuit of a three phase voltage source inverter*

The function of the PWM circuit can be described as

$$M_i = \begin{cases} V^+ & (\text{if } V_i - D_i > 0) \\ V^- & (\text{if } V_i - D_i < 0) \end{cases} \quad i = 1, 2, 3 \tag{18}$$

The ON/OFF state of the power transistors in the VSI can be described as

$$\begin{cases} T_i \equiv \text{ON} \\ T_{i+3} \equiv \text{OFF} \end{cases} \quad (\text{when } M_i = V^+, i = 1, 2, 3) \tag{19a}$$

and

$$\begin{cases} T_i \equiv \text{OFF} \\ T_{i+3} \equiv \text{ON} \end{cases} \quad (\text{when } M_i = V^-, i = 1, 2, 3) \tag{19b}$$

From Fig. 7 and eqn. 19, one obtains

$$V_{ap} = \begin{cases} V_{DC} & (\text{if } M_1 = V^+) \\ 0 & (\text{if } M_1 = V^-) \end{cases} \tag{20a}$$

$$V_{bp} = \begin{cases} V_{DC} & (\text{if } M_2 = V^+) \\ 0 & (\text{if } M_2 = V^-) \end{cases} \tag{20b}$$

and

$$V_{cp} = \begin{cases} V_{DC} & (\text{if } M_3 = V^+) \\ 0 & (\text{if } M_3 = V^-) \end{cases} \tag{20c}$$

The following phase voltage equations may be written from Fig. 7:

$$v_{ap} = v_{as} + v_{sp} \tag{21a}$$

$$v_{bp} = v_{bs} + v_{sp} \tag{21b}$$

$$v_{cp} = v_{cs} + v_{sp} \tag{21c}$$

The stator is connected as a three-wire system, where $i_{as} + i_{bs} + i_{cs} = 0$ and, from eqn. 1, one knows that the sum of v_{as}, v_{bs} and v_{cs} is also zero. Thus, by adding eqns. 21*a*, *b* and *c*, one obtains

$$v_{sp} = \tfrac{1}{3}(v_{ap} + v_{bp} + v_{cp}) \tag{21d}$$

Hence,

$$v_{as} = \tfrac{2}{3}\, v_{ap} - \tfrac{1}{3}(v_{bp} + v_{cp}) \tag{21e}$$

$$v_{bs} = \tfrac{2}{3}\, v_{bp} - \tfrac{1}{3}(v_{ap} + v_{cp}) \tag{21f}$$

$$v_{cs} = \tfrac{2}{3}\, v_{cp} - \tfrac{1}{3}(v_{ap} + v_{bp}) \tag{21g}$$

In the PWM circuit, if $V_1 = A_m \sin(\omega t)$, then the approximate phase voltage is [8]

$$V_{as} = \frac{V_{DC}\, A_m}{2A_d} \sin(\omega t)$$

where V_{DC} is the DC supply voltage in the VSI and A_d is the triangular peak value. Thus, the mode of the PWM circuit can be simplified as a constant gain

$$K_A = \frac{V_{as}}{V_1} = \frac{V_{DC}\, A_m}{2A_d} \tag{22}$$

The current loop is designed to achieve fast accurate current tracking. In this situation, the model of the current-controlled loop can be simplified to a single input single output (SISO) system as shown in Fig. 8 such that the conventional methods for analysing SISO systems may be applied with relative ease.

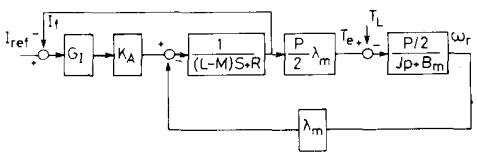

Fig. 8 *The simplified dynamic model of a current-controlled loop*

4.2 Design the IVSC

The simplified dynamic model of the brushless dc position control system with the integral variable structure controller is shown in Fig. 9. Based on this block diagram, one can obtain:

$$\dot{X}_1 = X_2 \tag{23a}$$

$$\dot{X}_2 = X_3 \tag{23b}$$

$$\dot{X}_3 = -a_2 X_2 - a_3 X_3 + bU - f(t) \tag{23c}$$

$$\dot{Z} = r - X_1 \tag{23d}$$

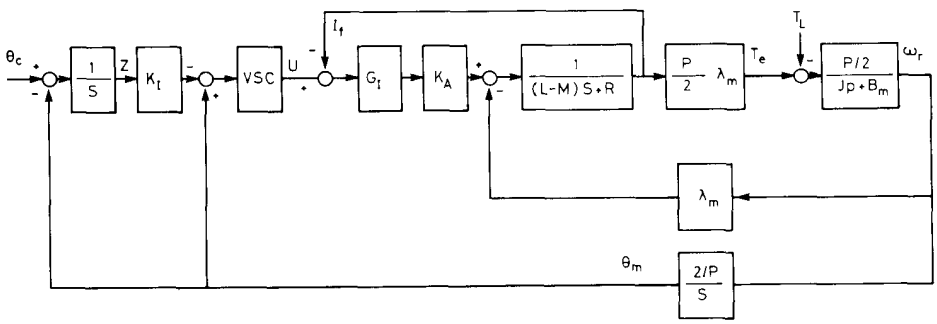

Fig. 9 *The simplified dynamic model of a brushless DC position control system with the integral variable structure controller*

where

$$a_2 = \frac{(R + G_I K_A)B_m + \frac{1}{2}P\lambda_m}{J(L - M)}$$

$$a_3 = \frac{(R + G_I K_A)}{L - M} + B_m$$

$$b = \frac{1}{2}P\lambda_m \frac{G_I K_A}{J(L - M)}$$

$$f(t) = \frac{(R + G_I K_A)}{J(L - M)} T_L + \frac{1}{J}\dot{T}_L$$

and where $X_1 = \theta_m$ is the mechanical angular position of the rotor, $r = \theta_c$ is the reference input, and K_I is the gain of the integral controller.

Following the design procedure as described in Section 3, one obtains

$$U = \{c_1 K_I(r - X_1) - c_1 X_2 + a_2^0 X_2(c_2 - a_3^0)[c_1(X_1 - K_I Z) + c_2 X_2]\}/b^0 + (\Psi_1|X_1 - K_I Z| + \Psi_2|X_2| + \Psi_3|X_3|) \times M_\delta(\sigma) \quad (24a)$$

where a_2^0, a_3^0 and b^0 are the nominal values, and Δa_2, Δa_3 and Δb are the associated variations, and

$$\Psi_i < |\Delta a_i - a_i^0 \Delta b/b^0 + c_{i-1}\Delta b/b^0 - c_i(c_{n-1} - a_n^0)(1 + \Delta b/b^0)|/b \quad i = 1, 2 \quad \text{and} \quad c_0 = 0 \quad (25a)$$

$$\Psi_3 < |\Delta a_3 + a_3 - c_2|/b \quad (25b)$$

The σ function, constructed from eqn. 5, is

$$\sigma = c_1(X_1 - K_I Z) + c_2 X_2 + X_3 \quad (26)$$

In the sliding motion, the system described by eqn. 23 can be reduced to the following simple linear form:

$$\dot{X}_1 = X_2 \quad (27a)$$

$$\dot{X}_2 = -c_1 X_1 - c_2 X_2 + c_1 K_I Z \quad (27b)$$

$$\dot{Z} = r - X_1 \quad (27c)$$

The characteristic equation of this reduced system is

$$S^3 + c_2 S^2 + c_1 S + c_1 K_I = 0 \quad (28)$$

It is clear that the dynamic performance of the system can now be determined by simply choosing the coefficients c_1, c_2 and the gain K_I. Let λ_1, λ_2 and λ_3 be the desired eigenvalues, which corresponds to a characteristic equation

$$S^3 - (\lambda_1 + \lambda_2 + \lambda_3)S^2 + (\lambda_1\lambda_2 + \lambda_1\lambda_3 + \lambda_2\lambda_3)S - \lambda_1\lambda_2\lambda_3 = 0 \quad (29)$$

Then c_1, c_2 and K_I can be chosen as

$$c_2 = -(\lambda_1 + \lambda_2 + \lambda_3) \quad (30a)$$

$$c_1 = (\lambda_1\lambda_2 + \lambda_1\lambda_3 + \lambda_2\lambda_3) \quad (30b)$$

$$K_I = \frac{-\lambda_1\lambda_2\lambda_3}{\lambda_1\lambda_2 + \lambda_1\lambda_3 + \lambda_2\lambda_3} \quad (30c)$$

5 Simulation results and discussions

Though the simplified dynamic model used for designing the IVSC is reasonable, the exact behaviour of the overall system can be understood through simulation of the model as shown in Fig. 5, including the IVSC, current control loop, PWM VSI as described in eqns. 18–21 and dynamics of the brushless dc motor as expressed in eqns. 1 and 2. The nominal values of the machine parameters are listed in Table 1. The robustness of the proposed IVSC approach against large variations of plant parameters and external load disturbance has been simulated for demonstration. The simulation results were compared to those obtained by a convention VSC and a linear controller.

Table 1: System parameters for simulation

Parmeter	Value	Dimension
P	4	pole
R	0.6	Ω
$L - M$	0.0015	H
λ_m	0.105	Vs/rad
J	2.84×10^{-4}	kg m^2
B_m	0.0	Nm/s
K_A	12.5	dimensionless
G_I	10.0	dimensionless
V_{DC}	150.0	V
A_d	6.0	V

Choosing the poles of the system, as described by eqn. 24, at -50 and $-45 \pm j22$, we obtain the coefficients of the switching plane and the integral control gain given by eqn. 30 as $c_1 = 7000$, $c_2 = 140$, and $K_I = 17.8$.

The gains Ψ_1,Ψ_2 and Ψ_3 must be chosen to satisfy eqn. 25 and, based on simulations, one possible set of the switching gains can be chosen as $\Psi_1 = -1$, $\Psi_2 = -0.001$, and $\Psi_3 = -0.00001$.

This IVSC design gives a control function

$$U = \{c_1 K_I(r - X_1) - c_1 X_2 + a_2^0 X_2 + (c_2 - a_3^0)[c_1(X_1 - K_I Z) + c_2 X_2]\}/b^0 + (\Psi_1|X_1 - K_I Z| + \Psi_2|X_2| + \Psi_3|X_3|)M_\delta(\sigma)$$

where $M_\delta(\sigma)$ is given by eqn. 19, $\sigma = 7000(X_1 - K_I Z) + 140X_2 + X_3$ and $\delta = 20000|X_1 - r| + 500$.

Two other approaches are presented here for performance comparison as follows:

(a) The conventional VSC approach

Let the control function U be

$$U = \{(a_2^0 - 1200)X_2 + (a_3^0 - 50)[-1200(X_1 - r) - 50X_2]\}/b^0 + (-10|X_1 - r| - 0.1|X_2| - 0.001|X_3|)M_\delta(\sigma)$$

where $\sigma = 1200(X_1 - r) + 50X_2 + X_3$, and $\delta = 200|X_1 - r| + 10$.

The control gain and the switching plane are chosen with the aims of matching the dynamic response of the proposed approach under no load situation.

(b) The conventional linear approach

The gains $G_1 = 40$, $G_2 = 40$, and $G_3 = 0.2$, as shown in Fig. 10, are chosen by means of computer-aided technique [9] to match the dynamic response of the IVSC approach under no load situation.

The simulation results of the dynamic responses are plotted in Fig. 11 to Fig. 14 under various operating conditions. Fig. 11 shows the dynamic responses of the three approaches when a shaft-angle-dependent external load disturbance T_L is present. It is clear that the loaded response of the IVSC approach can be maintained almost

identical to that of the no load situation, while vary significantly for both linear and VSC approaches. Fig. 12 shows the dynamic response of the three approaches under a constant external load disturbance. Results show that the IVSC approach converges very fast to zero state, but the others give rise to significant deviations and/or steady-state errors.

Fig. 13 shows the waveforms of the control function U. It is clear that by using a modified proper continuous function the chattering phenomena can be eliminated. Thus, the IVSC approach seems amenable for practical implementation.

Figs. 14 shows the dynamic responses of the three approaches under changes of the inertia J, and the damping coefficient B_m, respectively. From the observations, we conclude that the IVSC approach is very insensitive to the variations of the parameters J and B_m. This conclusion agrees with that predicted by the characteristic equation given by eqn. 29 which should be independent of the plant parameters.

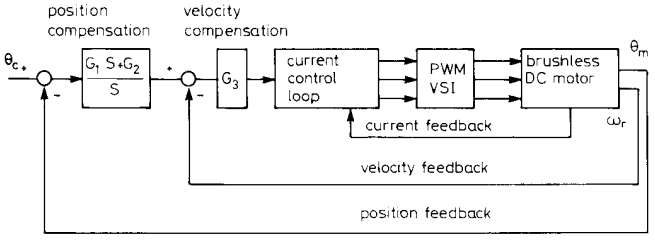

Fig. 10 *The block diagram of the brushless DC position control system with the conventional linear controller*

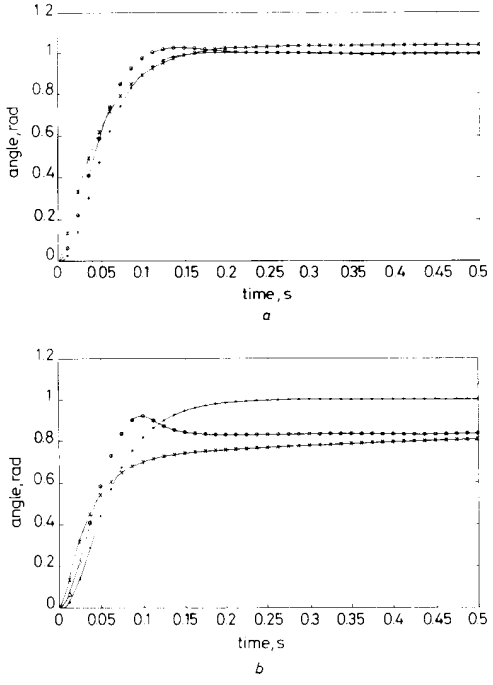

Fig. 11 *Angle responses of the IVSC, VSC, and linear approaches with a* $M_\delta(\sigma)$, $\delta = 500 + 20\,000\,|X_1 - \theta_c|$ *and input command* $\theta_c = 1$ *rad*

a $T_L = 0$ Nm
b $T_L = 0.5\,|\theta_m|$ Nm
—✱— IVSC
—○— VSC
× linear

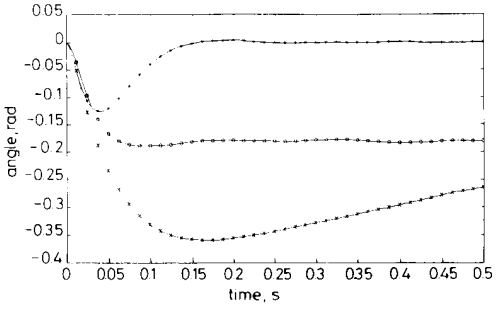

Fig. 12 *Angle responses of the IVSC, VSC and linear approaches with a* $M_\delta(\sigma)$, $\delta = 500 + 20\,000\,|X_1 - \theta_c|$ *input command* $\theta_c = 0$ *rad*

$T_L = 0.5$ Nm
—✱— IVSC
—○— VSC
—×··· linear

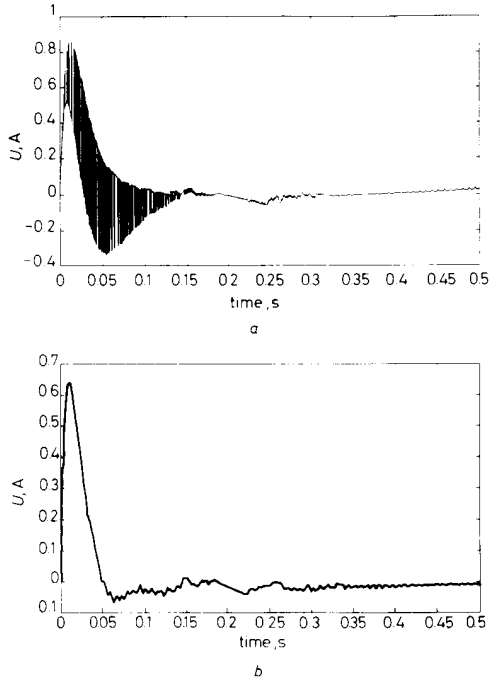

Fig. 13 *Control signal in the IVSC approach with* $\theta_c = 1$ *rad*

a without $M_\delta(\sigma)$, $\delta = 0$
b with $M_\delta(\sigma)$, $\delta = 500 + 20\,000\,|X_1 - \theta_c|$

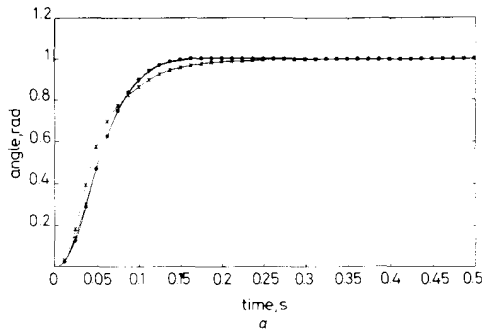

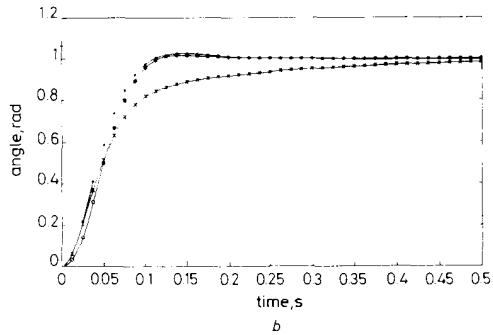

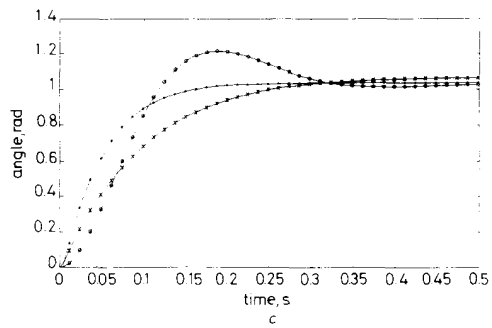

Fig. 14 *Angle responses of the IVSC, VSC and the linear approaches under changes of the inertia J and damping coefficient B_m*

a the IVSC approach
b the VSC approach
c the linear approach
—*— VSC (normal)
—○ VSC (1000% changes in *J*)
—× VSC (+0.05 changes in B_m)

6 Conclusions

An IVSC design methodology for the brushless DC servo position control system is presented. It has been shown that the IVSC approach is theoretically robust to the plant parameter variations. It can achieve a zero steady-state error for step input and is possible for arbitrary eigenvalue assignment. Simulations show that the proposed approach can give an almost accurate servo-tracking response in face of large plant parameter variations and external disturbances. It is a robust and practical law for the brushless DC servo control systems.

7 References

1 LOW, T.S., TSENG, K.J., LEE, T.H., LIM, K.W., and LOCK, K.S.: 'Strategy for the instantaneous torque control of permanent-magnet brushless DC drives', *IEE Proc. B*, 1990, **137**, pp. 355–363
2 UTKIN, V.I.: 'Variable structure systems with sliding modes', *IEEE Trans.*, 1977, **AC-22**, pp. 212–222
3 UTKIN, V.I.: 'Sliding modes and their application in variable structure system' (Mir, Moscow, 1978)
4 ITKIS, U.: 'Control systems of variable structure' (John Wiley, New York, 1976), p. 76
5 CHERN, T.L., and WU, Y.C.: 'Design of integral variable controller and application to electrohydraulic velocity servo systems', *IEE Proc. D.*, 1991, **138**, (5), pp. 439–444
6 CHERN, T.L., and WU, Y.C.: 'Integral variable structure control approach for robot manipulators', *IEE Proc. D.*, **139**, (2), pp. 161–166
7 KRAUSE, P.C., and WASYNCZUK, O.: 'Electromechanical motion devices' (McGraw-Hill, New York, 1989)
8 BROD, D.M., and NOVOTNY, D.W.: 'Current control of VSI-PWM inverters', *IEEE Trans.*, 1985, **IA-21**, (4), pp. 562–570
9 ASHWORTH, M.J., and TOWILL, D.R.: 'Computer-aided design of tracking systems', *Radio Electron. Eng.*, 1978, **48**, pp. 479–492